Available online at www.sciencedirect.com
ScienceDirect
ELSEVIER
Polymer 48 (2007) 6134–6144
polymer
www.elsevier.com/locate/polymer

Morphology and thermomechanical properties of nanostructured thermosetting blends of epoxy resin and poly(ε-caprolactone)-*block*-polydimethylsiloxane-*block*-poly(ε-caprolactone) triblock copolymer

Zhiguang Xu, Sixun Zheng*

Department of Polymer Science and Engineering, Shanghai Jiao Tong University, Shanghai 200240, PR China

Received 7 April 2007; received in revised form 24 June 2007; accepted 29 July 2007
Available online 6 August 2007

Abstract

Poly(ε-caprolactone)-*block*-polydimethylsiloxane-*block*-poly(ε-caprolactone) triblock copolymer (PCL-*b*-PDMS-*b*-PCL) was synthesized *via* the ring-opening polymerization of ε-caprolactone with dihydroxypropyl-terminated PDMS (HTPDMS) as the initiator. The triblock block copolymer was characterized by means of Fourier transform infrared spectroscopy (FTIR), nuclear magnetic resonance spectroscopy (NMR) and gel permeation chromatography (GPC). The triblock copolymer was incorporated to prepare nanostructured thermosetting blends. The morphology of the epoxy thermosets containing PCL-*b*-PDMS-*b*-PCL were investigated by means of atomic force microscopy (AFM), transmission electronic microscopy (TEM) and small-angle X-ray scattering (SAXS). The thermomechanical properties of the nanostructured blends were investigated by means of differential scanning calorimetry (DSC) and dynamic mechanical analysis (DMA). The formation of the nanostructures in the thermosetting composites was judged to follow the self-assembly mechanism in terms of the difference in miscibility of PDMS and PCL subchains with epoxy resin after and before curing reaction.

Keywords: PCL-*b*-PDMS-*b*-PCL triblock copolymer; Epoxy resin; Self-organized nanostructures

1. Introduction

Epoxy resins are a class of important thermosets and have widely been used as high performance materials such as adhesives, matrices of composites and electronic encapsulating materials [1,2]. Owing to high crosslinking density, epoxy resins are inherently of low impact resistance, which restricts their application. During the past decades considerable efforts have been made to improve toughness of epoxy thermosets [3–36]. One of the successful routines of toughness improvement is to incorporate polymeric modifiers into thermosetting matrix to form fine morphological structures. The effective polymer modifiers could be elastomers [3–15] or thermoplastics [16–31]. Liquid elastomers such as carboxyl-terminated butadiene–acrylonitrile rubber (CTBN), amine-terminated butadiene–acrylonitrile rubber (ATBN) [3–7] have been exploited to improve toughness of epoxy resins. However, the presence of unsaturated structure in CTBN and ATBN is prone to thermal instability and low oxidation resistance. In comparison, organosilicon polymers (*e.g.*, polydimethylsiloxane) are more advantageous modifiers [5,8–11,14], which possess some excellent properties, such as thermal stability, moisture resistance and good electrical properties. However, polysiloxanes have poor compatibility with the precursors of epoxy resin due to the big difference in solubility parameter [25], which is essential for the formation of fine phase-separated structures in thermosets [26].

In the conventional modification of thermosets with elastomers or thermoplastics, the control of morphology of materials is generally based on reaction-induced phase separation. Since the modifiers are some linear homopolymers or random copolymers, the modified thermosets would exhibit the

---

* Corresponding author. Tel.: +86 21 54743278; fax: +86 21 54741297.
E-mail address: szheng@sjtu.edu.cn (S. Zheng).

0032-3861/$ - see front matter © 2007 Elsevier Ltd. All rights reserved.
doi:10.1016/j.polymer.2007.07.072

phase-separated morphology on the macroscopic scale [37]. Recently, it is recognized that the formation of ordered (or disordered) nanostructures in thermosets could further optimize the interactions between thermoset matrix and modifiers and thus endow materials with improved properties [27–45]. Bates et al. [27,28] have proposed a strategy of creating nanostructures using amphiphilic block copolymers. In this protocol, the precursors of thermosets act as the selective solvents of block copolymers and some self-assembly microphases such as lamellar, bicontinuous, cylindrical, and spherical structures are formed in the mixtures depending on the blend composition before curing reaction. These nanostructures were further fixed with introduction of hardeners and subsequent curing. With an appropriate design of block copolymer architecture, the block copolymers self-assemble to form ordered or disordered nanostructures [29–49]. More recently, it is shown that the ordered (or disordered) nanostructures in the composite system of thermosets and amphiphilic block copolymers can be alternatively formed *via* so-called reaction-induced microphase separation mechanism [49–55].

Mülhaupt et al. [56,57] reported the modification of epoxy resin with a branched poly(ε-caprolactone)-*block*-polydimethylsiloxane-*block*-poly(ε-caprolactone) triblock copolymer. It is noted that the inclusion of a small amount of triblock copolymer (*e.g.*, 5 wt% or more) lead to a significant increase in toughness of materials whereas the strength of materials (*e.g.*, strength at break and Young's modulus) was not obviously reduced [56,57]. It was found that in the modified epoxy resin spherical PDMS particles with the size of about 20 nm in diameter are uniformly dispersed in the continuous epoxy matrix. However, the formation mechanism of the nanostructures was not clearly elucidated. More recently, Guo et al. [58] investigated the thermosetting blends of epoxy resin with poly(ethylene oxide)-*block*-polydimethylsiloxane diblock copolymer. It is proposed that the diblock copolymer behaved as a template to the formation of the nanostructured thermosets *via* self-assembly mechanism.

In the present work, we synthesized a linear triblock copolymer, poly(ε-caprolactone)-*block*-polydimethylsiloxane-*block*-poly(ε-caprolactone) (PCL-*b*-PDMS-*b*-PCL) *via* ring-opening polymerization (ROP) and this amphiphilic block copolymer was incorporated into epoxy thermosets to access the nanostructured thermosets. The morphology of the thermosets was investigated by means of atomic force microscopy (AFM), transmission electron microscopy (TEM) and small-angle X-ray scattering (SAXS). The formation mechanism of the nanostructures was addressed on the basis of the miscibility behavior of the blocks of the triblock copolymer with epoxy resin after and before curing reactions.

2. Experimental section

2.1. Materials

Diglycidyl ether of bisphenol A (DGEBA) with epoxide equivalent weight of 185–210 was purchased from Shanghai Resin Co., China. 4,4′-Methylenebis (2-chloroaniline) (MOCA) was used as the curing agent, obtained from Shanghai Reagent Co., China. The monomer of ε-caprolactone (CL) (Fluka, 99%) was dried over calcium hydride (CaH_2) and distilled under decreased pressure prior to use. Stannous octanoate [$Sn(Oct)_2$] was purchased from Aldrich Co., and used as the catalyst. The 3-hydroxylpropyl-terminated polydimethylsiloxane (HTPDMS, $M_n = 2600$) was kindly supplied by Th GoldSchmidt A.G., Germany. Before use, it was dried by azeotropic distillation with anhydrous toluene.

2.2. Synthesis of PCL-b-PDMS-b-PCL triblock copolymer

Poly(ε-caprolactone)-*block*-polydimethylsiloxane-*block*-poly(ε-caprolactone) triblock copolymer (PCL-*b*-PDMS-*b*-PCL) was synthesized *via* the ring-opening polymerization (ROP) of ε-CL in the presence of 3-hydroxypropyl-terminated PDMS (HTPDMS) with stannous octanoate as the catalyst. Typically, 3.7500 g (2.9 mmol with respect to hydroxyl groups of HTPDMS) polydimethylsiloxane, 9.8524 g (86.4 mmol) ε-CL and 1.3 mg $Sn(Oct)_2$ (in the solution of anhydrous toluene) were added to a 100 ml pre-dried round-bottom flask equipped with a magnetic stirrer. The flask was connected to a standard Schlenk line system and the pump-freeze-thaw cycle was repeated for three times to eliminate moisture. The flask was immersed into a thermostated oil bath at 120 °C to initiate the ring-opening polymerization. After the polymerization was carried out for 48 h, the system was cooled to room temperature and tetrahydrofuran was added. The solution was dropped into a great amount of petroleum ether to afford the precipitates. The polymer was dried in a vacuum oven at 40 °C until a constant weight (13.0200 g) was obtained with the yield of 94%. The FTIR (KBr window, cm^{-1}): 2943 (C–H, methylene of PCL), 1725 ($>$C=O, ester of PCL); 800 (Si–C, methyl of PDMS), 1097 (Si–O, main chain of PDMS). The ^1H NMR ($CDCl_3$, ppm): 4.04–4.07 [$OCO(CH_2)_4CH_2$, 4*H*], 2.28–2.32 [$OCOCH_2(CH_2)_4$, 4*H*], 1.60–1.68 [$OCOCH_2CH_2CH_2CH_2CH_2$, 8*H*], 1.35–1.41 [$OCOCH_2CH_2CH_2CH_2CH_2$, 4*H*]; 0.48–0.55 [$SiCH_2CH_2CH_2$, 0.07*H*], 0.03–0.09 [$Si(CH_3)_2$, 3.6*H*]. In views of the ratio of the integration intensity of PDMS protons to that of PCL, the molecular weight of copolymer was calculated to be $M_n = 9100$. The curve of gel permeation chromatography (GPC, relative polystyrene standard) displayed an unimodal peak and the molecular weight of $M_n = 10{,}800$ and $M_w/M_n = 1.12$ were determined relative to polystyrene standard.

2.3. Preparation of nanostructured epoxy resin

The desired amount of PCL-*b*-PDMS-*b*-PCL triblock copolymer was added to DGEBA with continuous stirring at 100 °C until the mixtures became homogenous and transparent. 4,4′-Methylene bis(2-chloroaniline) (MOCA) was added with continuous stirring until the full dissolution of the curing agent. The mixtures were poured into Teflon molds and cured at 150 °C for 2 h plus 180 °C for 2 h.

3. Measurement and characterization

3.1. Fourier transform infrared spectroscopy (FTIR)

FTIR spectra were measured by a Perkin-Elmer Paragon 1000 Fourier transform spectrometer. The block copolymer was dissolved in THF and then the solution was cast onto KBr windows. The solvent was evaporated *in vacuo* at 60 °C to obtain the specimen of films. For the samples of thermosets, the powder was mixed with KBr pellets to press into small flakes. All the specimens were sufficiently thin to be within a range where the Beer–Lambert law is obeyed. In all cases 64 scans at a resolution of 2 cm^{-1} were used to record the spectra.

3.2. Nuclear magnetic resonance spectroscopy (NMR)

The triblock copolymer was dissolved in deuterated chloroform and the NMR measurements were carried out in a Varian Mercury Plus 400 MHz NMR spectrometer with tetramethylsilane (TMS) as an internal reference.

3.3. Atomic force microscopy (AFM)

The samples of thermosets were trimmed using a microtome machine and the specimen sections (*ca.*, 70 nm in thickness) were used for AFM observations. The AFM experiments were performed with a Nanoscope IIIa scanning probe microscope (Digital Instruments, Santa Barbara, CA). Tapping mode was employed in air using a tip fabricated from silicon (125 μm in length with *ca.*, 500 kHz resonant frequency). Typical scan speeds during recording were 0.3–1 line × s^{-1} using scan heads with a maximum range of 16 × 16 μm.

3.4. Transmission electron microscopy (TEM)

Transmission electron microscopy was performed on a JEOL JEM-2010 high resolution transmission electron microscope at an acceleration voltage of 120 kV. The samples were trimmed using an ultramicrotome machine equipped with a diamond knife and then the ultrathin sections (*ca.*, 70 nm) were placed on 200 mesh copper grids for observation.

3.5. Small-angle X-ray scattering (SAXS)

The SAXS measurements were taken on a Bruker Nanostar system. Two dimensional diffraction patterns were recorded using an image intensified CCD detector. The experiments were carried out at room temperature (25 °C) using Cu Kα radiation ($\lambda = 1.54$ Å, wavelength) operating at 40 kV, 35 mA. The intensity profiles were output as the plot of scattering intensity (I) versus scattering vector, $q = (4/\lambda)\sin(\theta/2)$ (θ = scattering angle).

3.6. Dynamic mechanical thermal analysis (DMTA)

The dynamic mechanical tests were carried out on a dynamic mechanical thermal analyzer (DMTA) (Netzsch DMA242, Germany) in a single cantilever mode. The frequency used is 1.0 Hz and the heating rate is 3.0 °C/min. The specimen dimension was $25 \times 5.0 \times 2.0\ \text{mm}^3$. The experiments were carried out from −150 °C until the samples became too soft to be tested.

4. Results and discussion

4.1. Synthesis of PCL-b-PDMS-b-PCL triblock copolymer

Using ring-opening polymerization of ε-caprolactone with various hydroxyl-terminated PDMS as initiators, the preparations of PCL-*b*-PDMS-*b*-PDMS have previously been reported [56,57]. In the present work, the ring-opening polymerization of ε-caprolactone was carried out with dihydroxylpropyl-terminated PDMS as the initiator and stannous octanoate [Sn(Oct)_2] as the catalyst as shown in Scheme 1. This polymerization was carried out at 120 °C for 48 h to obtain a complete conversion of the monomer. Shown in Fig. 1 are the FTIR spectra of the PCL-*b*-PDMS-*b*-PCL triblock copolymer and HTPDMS. In the FTIR spectrum of HTPDMS, the absorption band at 1079 cm^{-1} is assignable to the stretching vibration of Si–O bonds of this polymer. It is seen that this band also appeared in the FTIR spectrum of the as-synthesized product, which indicates the presence of polydimethylsiloxane subchain in the polymer. In addition, the stretching vibration of carbonyl groups is seen at 1725 cm^{-1}, which is ascribed to the ester structural unit in PCL subchain. Fig. 2 presents the ^{1}H NMR spectrum of the triblock copolymer. As indicated in the ^{1}H NMR spectrum, the simultaneous appearance of the resonance characteristic of PCL and PDMS protons indicates that the resulting product combines the structural features of PCL and PDMS, *i.e.*, the PCL-*b*-PDMS-*b*-PCL triblock copolymer was successfully obtained. From the ratio of the integration intensities of PCL to those of PDMS protons in the ^{1}H NMR spectrum, the molecular weight of the triblock copolymer was calculated to be $M_n = 9100$. Therefore, the lengths of the subchains of the triblock copolymer are $M_n = 6500$ for PCL subchain and $M_n = 2600$ for PDMS subchain, respectively. This estimation of molecular weight is consistent with the result of gel permeation chromatography (GPC). The GPC curve of the polymer is shown in Fig. 3. The GPC trace of the product displayed an unimodal peak, indicating that the triblock copolymer was successfully prepared. The molecular weight of $M_n = 10{,}800$ together with $M_w/M_n = 1.12$ were determined relative to polystyrene standard.

4.2. Morphology of thermosets containing PCL-b-PDMS-b-PCL

Before curing, all the mixtures of the epoxy precursors (DGEBA and MOCA) and PCL-*b*-PDMS-*b*-PCL triblock copolymer were homogenous and transparent at room and elevated temperatures. This observation is in marked contrast to the mixture of the epoxy precursors with HTPDMS. The clarity suggests that the presence of miscible PCL blocks

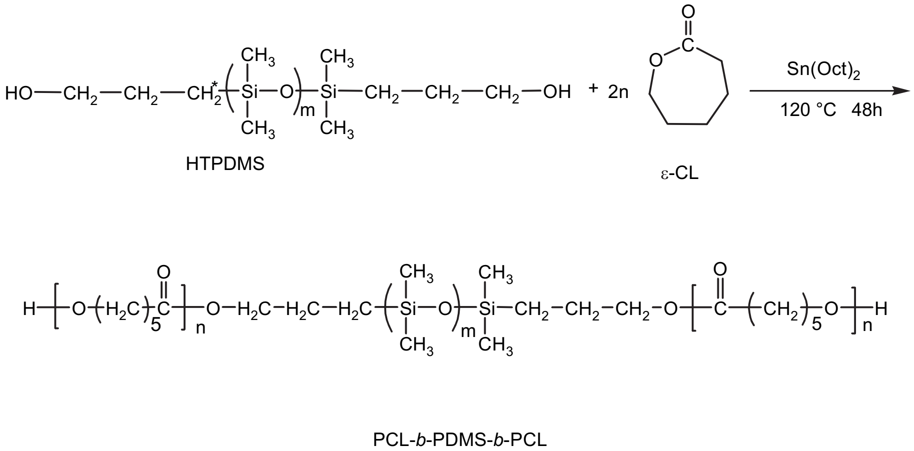

Scheme 1. Synthesis of PCL-*b*-PDMS-*b*-PCL triblock copolymer.

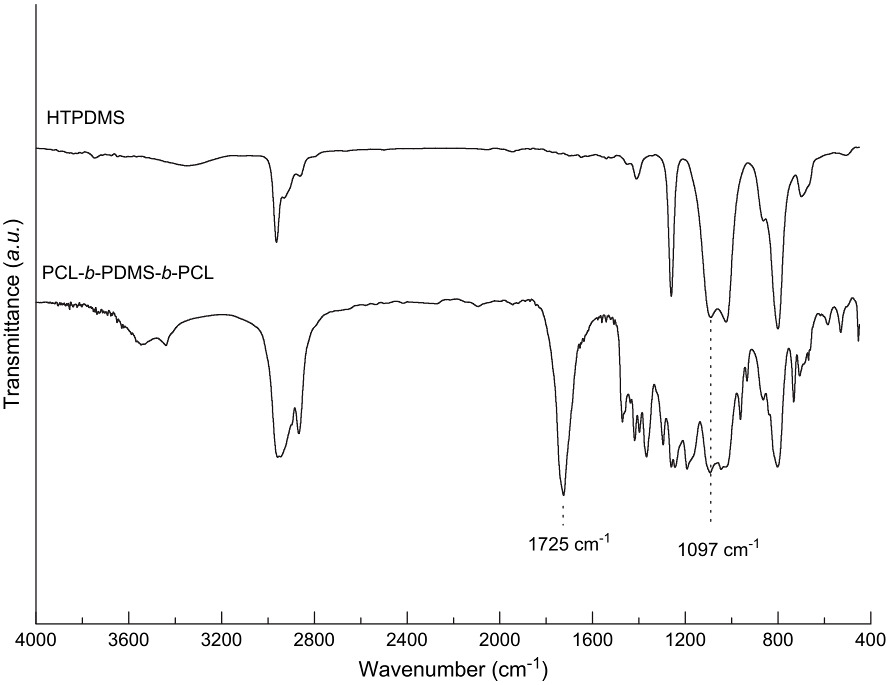

Fig. 1. FTIR spectrum of PCL-*b*-PDMS-*b*-PCL triblock copolymer.

connected to PDMS chain improves the dispersion of PDMS chains in the mixtures. With curing at 150 °C for 2 h plus 180 °C for 2 h, the thermosetting blends of epoxy resin with PCL-*b*-PDMS-*b*-PCL were obtained with the content of PCL-*b*-PDMS-*b*-PCL up to 40 wt%. It is seen that all the thermosets containing PCL-*b*-PDMS-*b*-PCL triblock copolymer are transparent and homogenous, suggesting that no macroscopic phase separation occurred at least on the scale exceeding the wavelength of visible light. The morphology of the epoxy thermosets was examined by means of transmission electronic microscopy (TEM) and atomic force microscopy (AFM).

Shown in Fig. 4 are the TEM micrographs of the thermosets containing PCL-*b*-PDMS-*b*-PCL triblock copolymer. The dark regions are attributed to the domains of PDMS whereas the light to epoxy matrix. It is seen that spherical PDMS particles with the size of ~20 nm were homogeneously dispersed into the continuous epoxy matrix (Fig. 4a). With increasing the content of the triblock copolymer, the spherical nanoparticles began to coagulate in the continuous epoxy matrix, and some wormlike nanodomains of PDMS appeared; the epoxy thermosets possessed a combined morphology, in which both spherical PDMS domains and some interconnected PDMS domains were present (Fig. 4b and c). The TEM results indicate that the epoxy thermosets possess the microphase-separated morphology. The nanostructures of the epoxy thermosets were further investigated by means of atomic force microscopy (AFM). The AFM images of the thermosets containing 10, 20, 30 and 40 wt% of the triblock copolymer PCL-*b*-PDMS-*b*-PCL are presented in Fig. 5. Shown in the left-hand side of each micrograph is the topography image and the right is the phase

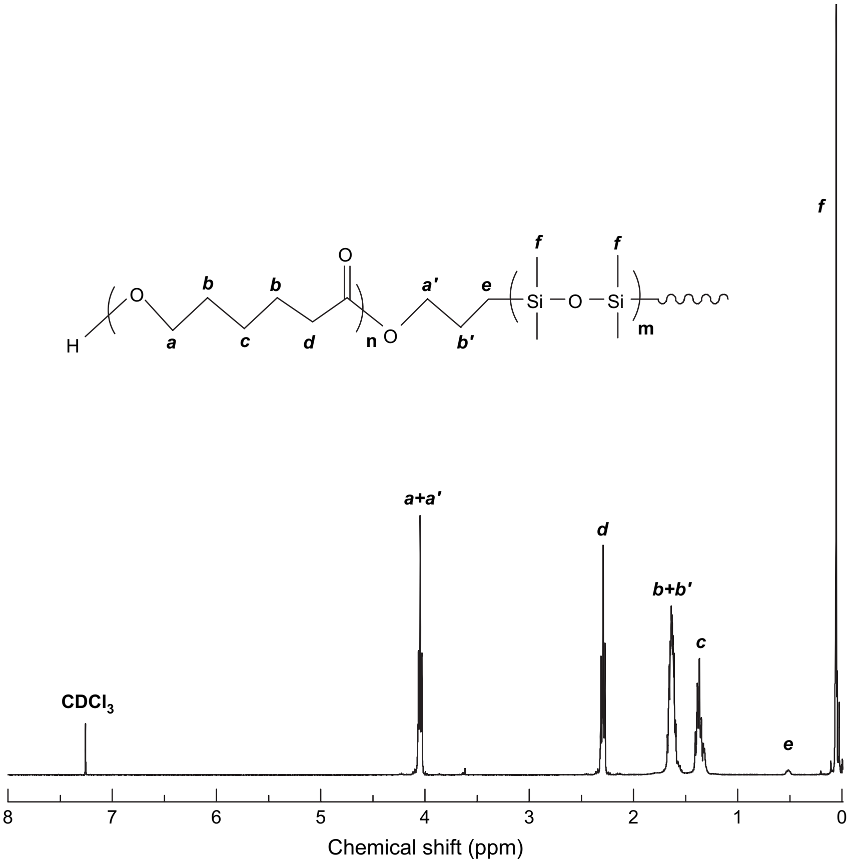

Fig. 2. The ^{1}H NMR spectrum of PCL-*b*-PDMS-*b*-PCL triblock copolymer.

image. The topography images show that the surfaces of the as-prepared specimens are free of visible defects and quite smooth and thus the effect of roughness resulting from the specimen trimming on morphology can be negligible. It is noted that all the blends exhibited nanostructured morphology. In terms of the volume fraction of PDMS and the difference in viscoelastic properties between epoxy and PDMS phases, the light continuous regions are ascribed to the epoxy matrix, which could be interpenetrated by the PCL blocks of the copolymer whilst the dark regions are attributed to PDMS domains. It is observed that the spherical PDMS nanoparticles with the size of 10–20 nm were homogenously dispersed into the continuous epoxy matrix and the sizes of the dispersed PDMS particles increased with increase in the content of PCL-*b*-PDMS-*b*-PCL in the thermosets (see Fig. 5a–d).

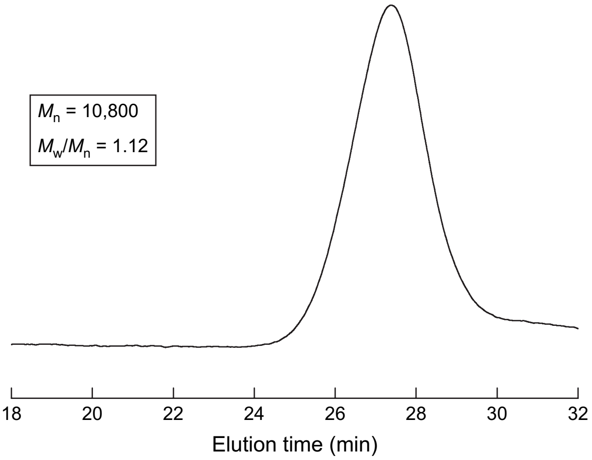

Fig. 3. The gel permeation chromatography (GPC) curves of PCL-*b*-PDMS-*b*-PCL triblock copolymer.

The morphologies of the thermosetting blends were further investigated by small-angle X-ray scattering (SAXS) and the SAXS profiles are shown in Fig. 6. It is seen that the well-defined scattering peaks were observed in all the cases, indicating that the thermosets containing PCL-*b*-PDMS-*b*-PCL are nanostructured. According to the position of the primary scattering peaks the average distance ($L = 2\pi/q_m$) between neighboring domains can be estimated to be 25.7, 22.6, 20.8, and 19.0 nm for the thermosets containing the triblock copolymer of 10, 20, 30 and 40 wt%, respectively. It is seen that the average distance between neighboring domains decreased with increasing the content of the triblock copolymer. These results are in good agreement with those obtained by means of TEM and AFM.

4.3. Thermomechanical properties of nanostructured thermosets

The above nanostructured epoxy thermosets containing PCL-*b*-PDMS-*b*-PCL triblock copolymer were subjected to

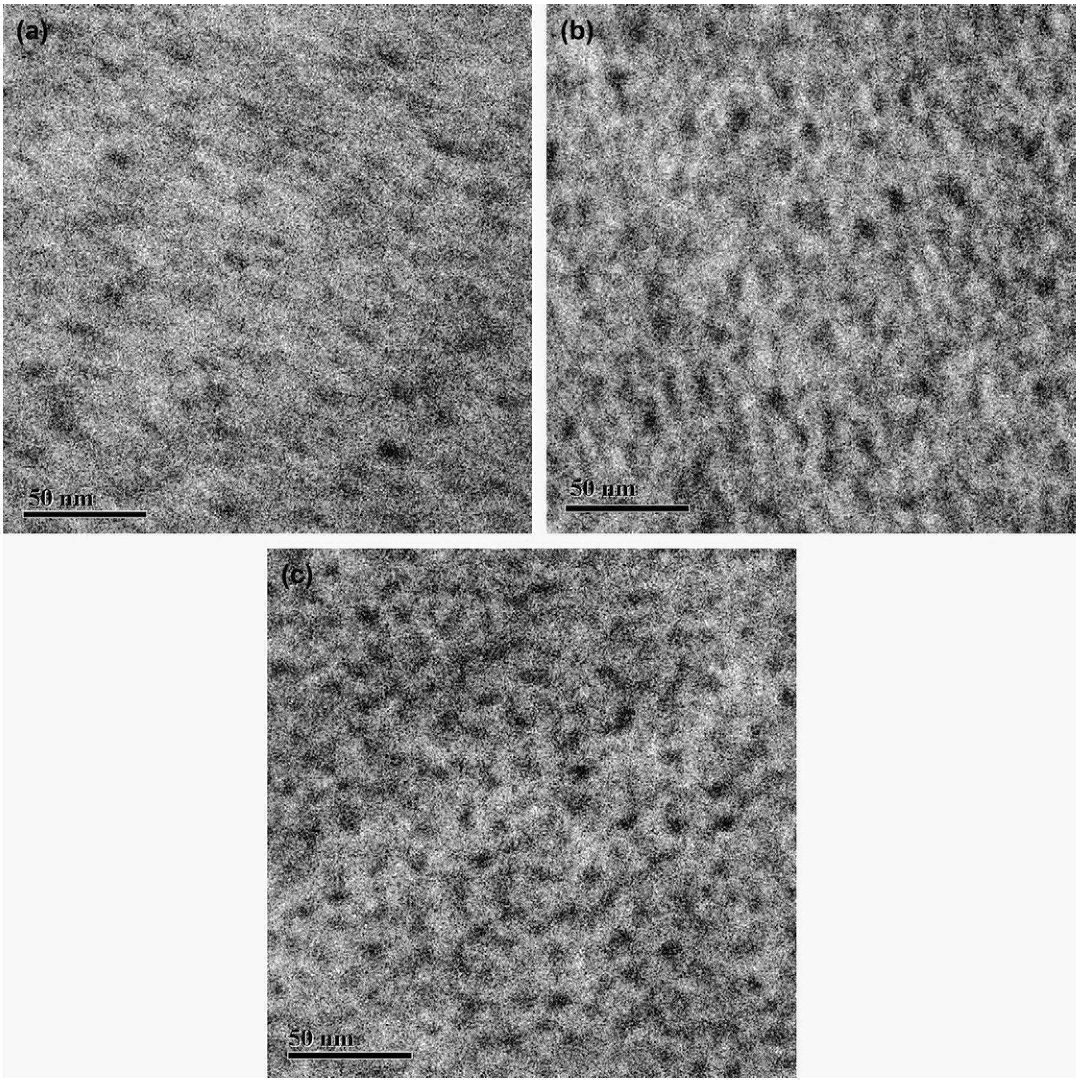

Fig. 4. The TEM micrographs of the nanostructured thermosets containing (a) 10, (b) 20, and (c) 30 wt% of PCL-*b*-PDMS-*b*-PCL block copolymer.

thermal analysis. Shown in Fig. 7 are the DSC curves of the thermosetting blends. The triblock copolymer PCL-*b*-PDMS-*b*-PCL displayed a sharp endothermic peak at 54 °C, which is assignable to the melting transition of the PCL blocks. It is noted that all the nanostructured thermosets containing the triblock copolymer did not exhibit the melting transition of PCL, suggesting that the PCL subchains in the thermosets are not crystallizable. It is proposed that the PCL subchains were miscible with aromatic amine-cured epoxy matrix and were interpenetrated with the crosslinked epoxy networks. The behavior of miscibility can also be evidenced by the depression of the glass temperatures (T_gs) of epoxy matrix. It is seen that the T_gs of the nanostructured thermosets are decreased with increasing the concentration of the triblock copolymer. The decreased T_g is responsible for the plasticization effect of the PCL blocks on the epoxy matrix. This result is in good agreement with the result that the MOCA-cured epoxy resin is miscible with PCL [59,60]. It should be pointed out that the glass transition observed in the present temperature range is only ascribed to the epoxy matrix which is interpenetrated with the PCL subchains of the block copolymers since the T_g of PDMS domains (~ -120 °C) is beyond the temperature range of the DSC measurement.

The nanostructured thermosets containing PCL-*b*-PDMS-*b*-PCL were further subjected to dynamic mechanical analysis (DMA). Shown in Fig. 8 are the dynamic mechanical spectra of the nanostructured epoxy thermosets. The MOCA-cured epoxy exhibited a well-defined major relaxation peak centered at *ca.*, 148 °C, which is responsible for the glass–rubber transition of the crosslinked polymer. Apart from the α transition, the MOCA-cured epoxy exhibited a secondary transition at the lower temperature (~ -50 °C). This transition is attributed predominantly to the motion of hydroxyl ether structural units [$-CH_2-CH(OH)-CH_2-O-$] and diphenyl groups in amine-crosslinked epoxy [61–63]. It is seen that upon adding PCL-*b*-PDMS-*b*-PCL into the thermosets, the α transition shifted to the lower temperatures and the T_g of epoxy matrix decreased with increasing the content of PCL-*b*-PDMS-*b*-PCL diblock copolymer. The decreased T_gs are ascribed to the

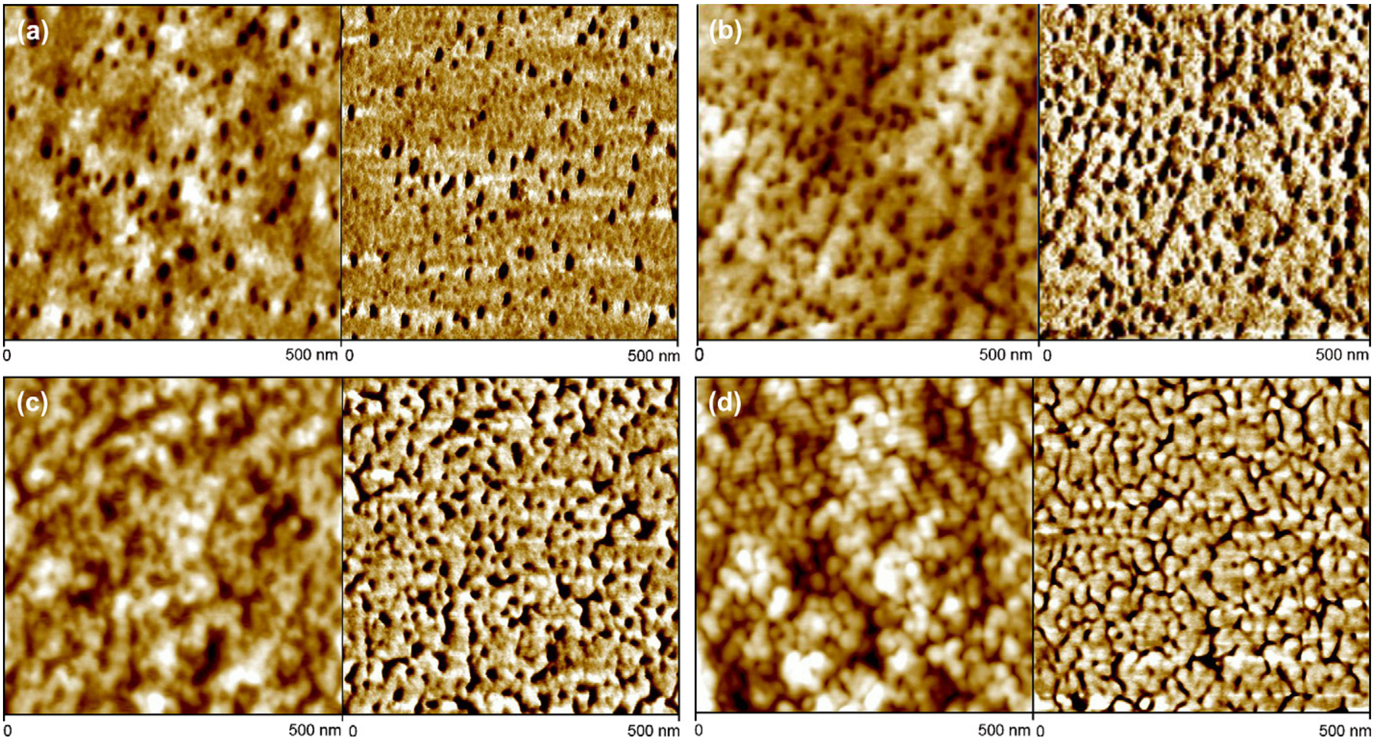

Fig. 5. The AFM images of the epoxy thermosets containing (a) 10, (b) 20, (c) 30, and (d) 40 wt% of PCL-*b*-PDMS-*b*-PCL triblock copolymer. Left: topography; right: phase contrast images.

plasticization of PCL subchains of the block copolymer on the epoxy matrix. It is noted that the α transition of PDMS nanodomains is not pronounced until the content of PCL-*b*-PDMS-*b*-PCL triblock copolymers is more than 30 wt%. It is seen that the T_g of the PDMS nanophases for the thermoset containing 30 wt% PCL-*b*-PDMS-*b*-PCL is about −117 °C (see Fig. 9). The DMA results indicate that the epoxy thermosets containing PCL-*b*-PDMS-*b*-PCL are microphase-separated.

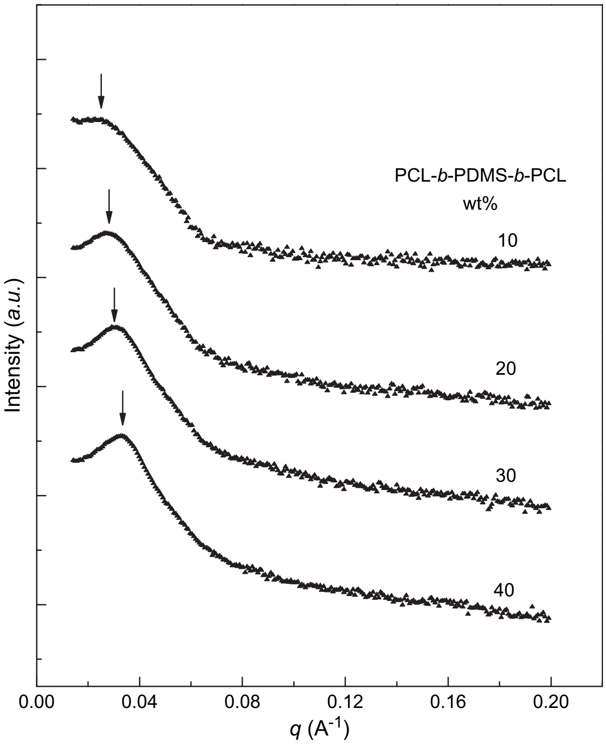

Fig. 6. The SAXS profiles of the epoxy thermosets containing PCL-*b*-PDMS-*b*-PCL triblock copolymer.

4.4. Formation mechanism of nanostructures

The formation of nanostructures in thermosets containing amphiphilic block copolymers could follow the following two mechanisms: (i) self-assembly [27–49], (ii) reaction-induced microphase separation [51–55]. In the mechanism of self-assembly, the precursors of thermosets act as selective solvents of block copolymers and self-organized nanostructures (*i.e.*, micelle) are formed prior to curing. These disordered and/or ordered nanostructures can further be fixed with the subsequent curing reaction. In this method, the role of curing reaction is to lock the preformed morphology [27,28]. The prerequisite for the self-assembly approach is that block copolymers are self-organized into micelle structures in their mixtures with precursors of thermosets prior to curing. From the viewpoint of miscibility, it is required that one or more of subchains of block copolymers are immiscible whereas other subchains are miscible with thermosets after and before curing. For the formation of nanostructures *via* reaction-induced microphase separation mechanism, it is required that all the subchains of the block copolymer are miscible with precursors of thermosets whereas only a part of subchains was separated out from the matrix of thermosets after curing. Therefore, it is crucial to know the miscibility of all

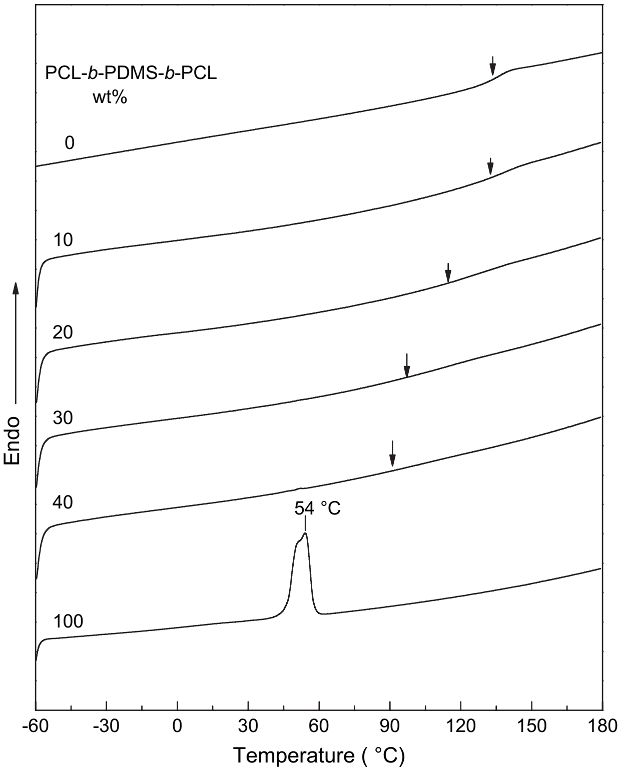

Fig. 7. The DSC curves of the nanostructured epoxy thermosets.

the subchains with thermosets after and before curing reaction for the judgment of the formation mechanism of the nanostructures in thermosets containing amphiphilic block copolymers.

In the present work, it has been known that the PCL subchain of the PCL-*b*-PDMS-*b*-PCL triblock copolymer is miscible with the precursors of epoxy resin (*viz.* DGEBA and MOCA) and also miscible with epoxy thermosets after curing [59,60]. Fourier transform infrared spectroscopy (FTIR) showed that there were the intermolecular specific interactions (*i.e.*, hydrogen-bonding) between PCL chains and epoxy matrix. As for the binary blends of epoxy resin with PDMS, it is recognized that the systems are immiscible after and before curing reaction [29]. The immiscibility could be responsible for the big difference in solubility parameter between epoxy resin and the inorganic polymer. The difference in miscibility between the two kinds of subchains (*viz.* PCL and PDMS) of the triblock copolymers with the precursors of epoxy resin result in the formation of some self-organized microstructures in the mixtures of PCL-*b*-PDMS-*b*-PCL and the precursors of epoxy resin (DGEBA and MOCA). Therefore, the formation of nanostructures in the present thermosetting system could follow the self-assembly mechanism other than the reaction-induced microphase separation mechanism. It is proposed that the self-organized nanostructures in the mixtures of PCL-*b*-PDMS-*b*-PCL and the precursors of epoxy resin (*viz.* DGEBA and MOCA) are formed before curing reaction due to the immiscibility of PDMS blocks and the miscibility of PCL blocks with the precursors. The nanostructures are reserved until the completion of the curing reaction. This judgment can be demonstrated by investigating the microphase structures by means of small-angle X-ray scattering (SAXS). Fig. 10 representatively presents the SAXS profiles of the mixture of epoxy resin with PCL-*b*-PDMS-*b*-PCL (10 wt%). At room temperature, the SAXS curve displays a scattering shoulder at $q = 0.04\ \mathrm{nm}^{-1}$, corresponding to a long period of 15.7 nm (see curve a). The flat scattering shoulder other than a scattering maximum implies that the size distribution of the self-organized nanoobjects in the mixtures could be quite broad. Nonetheless, the SAXS results indeed indicate that the system possesses microphase-separated structure before curing reaction. It was worth noticing that when the mixture was heated to 150 °C (*i.e.*, curing temperature), the intensity of the scattering shoulder was significantly decreased, indicating that the self-organized structures could be to some extent destroyed at elevated temperature. This observation suggests that there is partial miscibility between the PDMS subchain of the triblock copolymer with the precursors of epoxy resin at elevated temperature. With the occurrence of the curing reaction at 150 °C for 4 h, it is seen that a well-defined scattering peak appeared (see curve c). The well-defined scattering peak suggests that the occurrence of curing reaction promotes the narrow size distribution of PDMS nanoobjects. According to Bragg equation, the long period was estimated to be *ca.*, 25.7 nm, which is quite higher than that of the value obtained before curing reaction (*i.e.*, *ca.*, 15.7 nm). This observation could be responsible for the effect of curing reaction on the morphology. Prior to cure, the domain of PDMS could be swollen by the precursors of epoxy and thus the smaller distances between adjacent PDMS domains. Upon curing at elevated temperature, the precursors of epoxy resin that swell the PDMS domains were extracted due to the formation of cross-linked polymer. Therefore, the average distances between the neighboring spherical domains were increased.

It should be pointed out that the PCL subchains of the triblock copolymer remained miscible with the MOCA-cured epoxy resin. The miscibility could be ascribed to the formation of the intermolecular specific interactions between PCL and the epoxy matrix. The intermolecular hydrogen-bonding interactions can readily be evidenced by Fourier transform infrared spectroscopy (FTIR). Shown in Fig. 11 are the FTIR spectra of PCL-*b*-PDMS-*b*-PCL triblock copolymer and the nanostructured epoxy thermosets in the range of $1800-1660\ \mathrm{cm}^{-1}$. The absorption band in this range is ascribed to the stretching vibration of carbonyl groups. For the PCL-*b*-PDMS-*b*-PCL at the room temperature, it is seen that the FTIR spectrum is composed of two components. The one component at $1735\ \mathrm{cm}^{-1}$ is assignable to the amorphous chains of PCL while another at $1725\ \mathrm{cm}^{-1}$ is ascribed to the carbonyls in the crystalline region of PCL. In the nanostructured thermosets, it is noted that the band assignable to crystalline region of PCL disappeared; instead the new shoulder bands at the lower frequency ($1706\ \mathrm{cm}^{-1}$) appeared. The shoulder band is ascribed to the stretching vibration of the carbonyl groups which are hydrogen-bonded with the secondary hydroxyl groups of MOCA-cured epoxy resins. In addition, it is noted

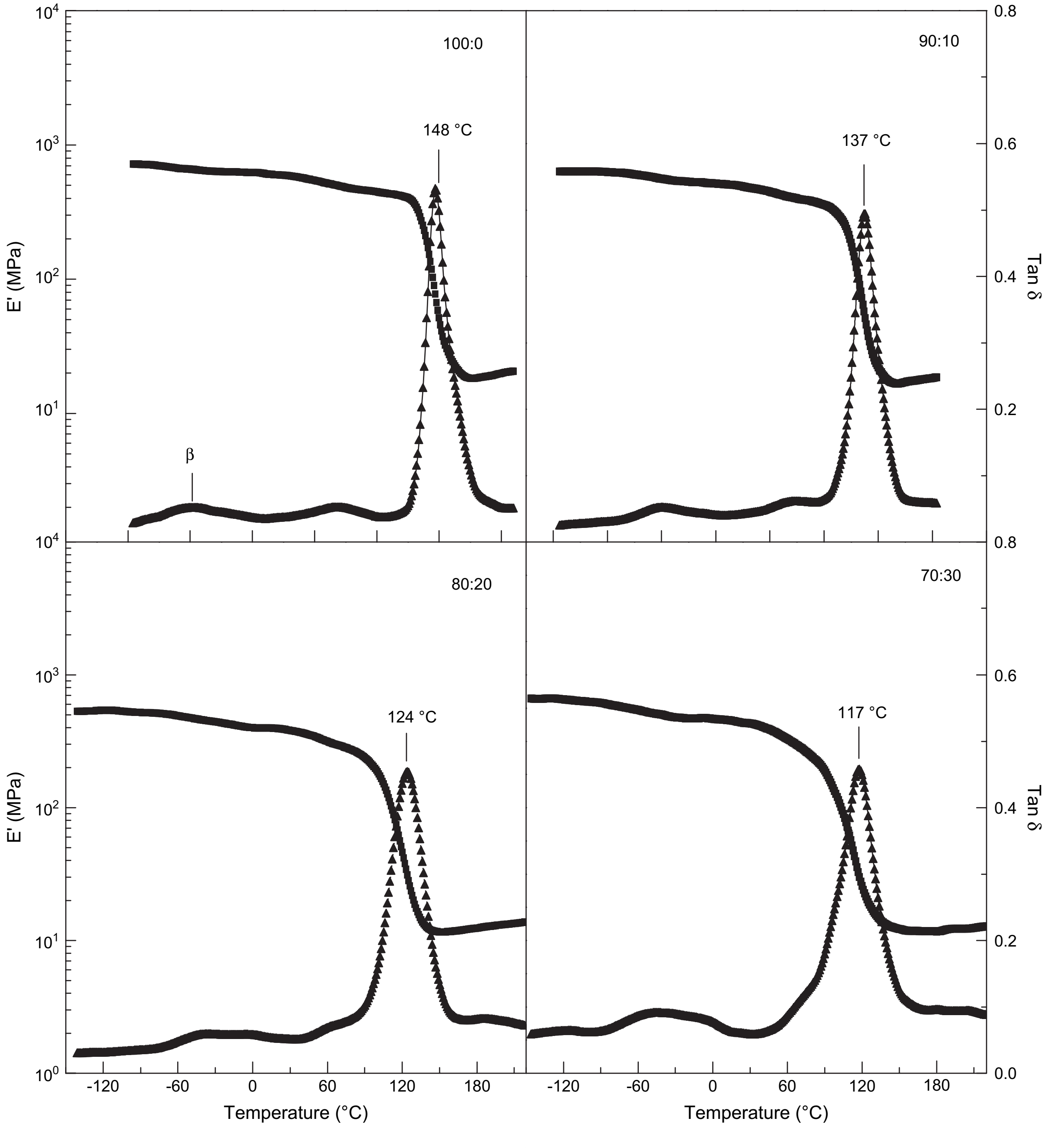

Fig. 8. The dynamic mechanical spectra of epoxy and the nanostructured thermosets.

that the band at 1731 cm^{-1} shifted to the higher frequency 1734 cm^{-1} with increasing the concentration of the triblock copolymer. The FTIR results indicated that the intermolecular hydrogen-bonding interactions were formed between the carbonyl of PCL subchains and the hydroxyl groups of crosslinked epoxy.

5. Conclusions

PCL-*b*-PDMS-*b*-PCL triblock copolymer was synthesized *via* the ring-opening polymerization of ε-caprolactone in the presence of dihydroxypropyl-terminated PDMS (HTPDMS). The triblock block copolymer was characterized by means of Fourier transform infrared spectroscopy (FTIR), nuclear magnetic resonance spectroscopy (NMR) and gel permeation chromatography (GPC). The amphiphilic triblock copolymer was incorporated into epoxy resin and the nanostructured thermosets were successfully obtained. The morphology of the epoxy thermosets containing PCL-*b*-PDMS-*b*-PCL triblock copolymers were investigated by means of atomic force microscopy (AFM), transmission electronic microscopy (TEM) and small-angle X-ray scattering (SAXS). The thermomechanical properties of the nanostructured thermosets were investigated by means of differential scanning calorimetry (DSC), dynamic mechanical analysis (DMA). The formation was judged to follow the self-assembly mechanism

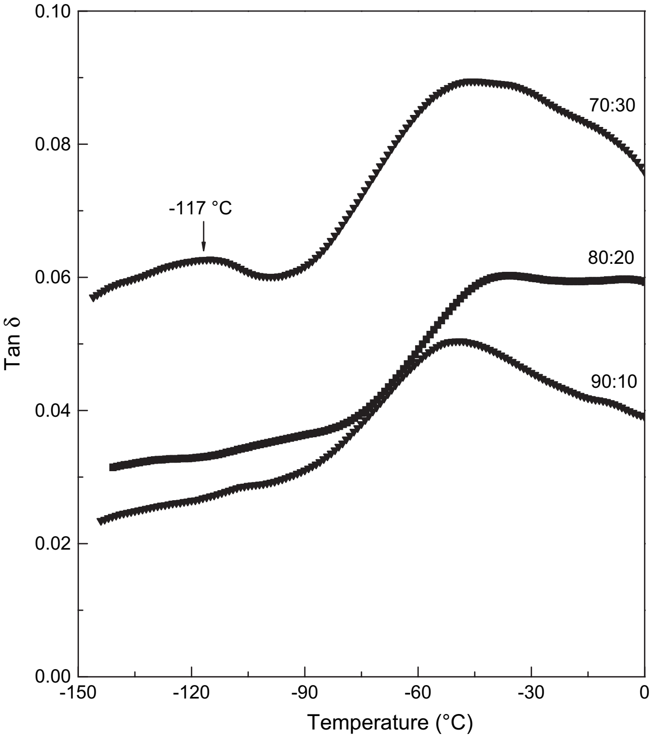

Fig. 9. The expanded dynamic mechanical spectra of the nanostructured epoxy thermosets in the range of −150–0 °C.

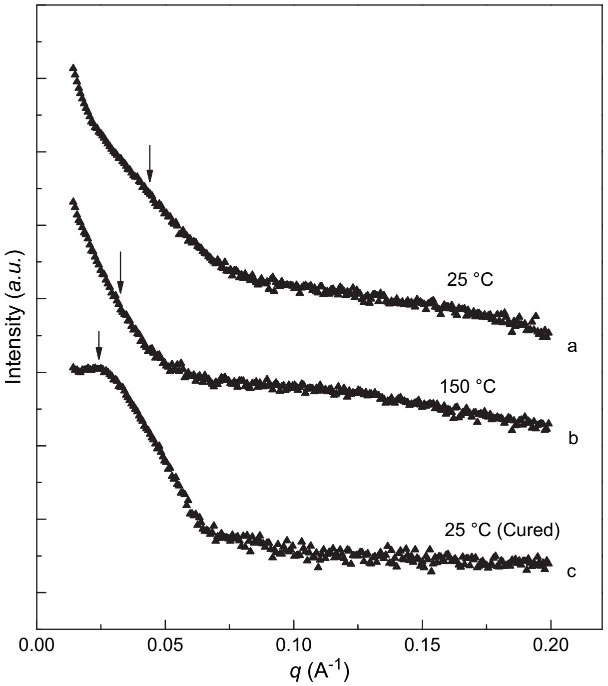

Fig. 10. The SAXS profiles of the blends of epoxy precursors with MOCA and 10 wt% PCL-*b*-PDMS-*b*-PCL: (a) at room temperature (25 °C); (b) at 150 °C at the beginning of curing reaction and (c) cured thermoset.

in terms of the difference in miscibility of the PDMS and PCL subchains with epoxy resin after and before curing reaction.

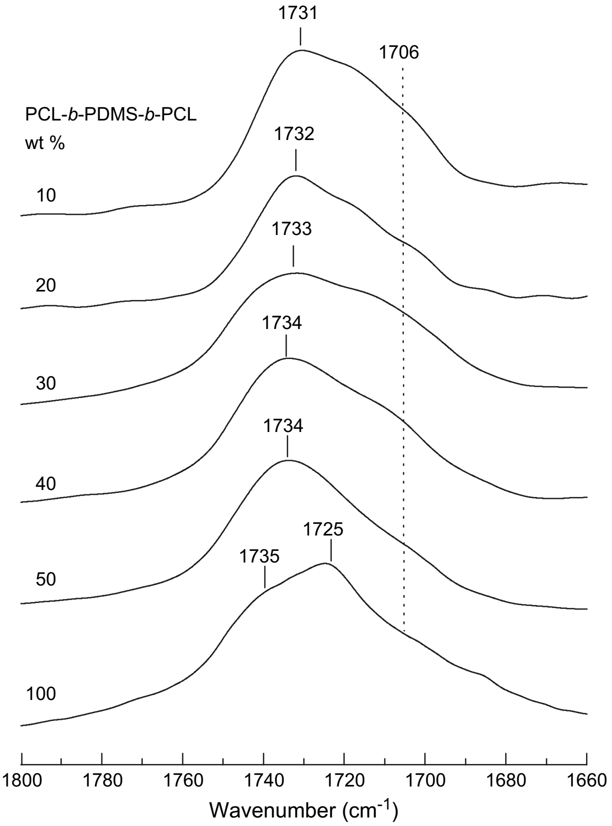

Fig. 11. The FTIR spectra of the nanostructured thermosets in the range of 1800–1660 cm^{-1}.

Acknowledgment

The financial support from the Natural Science foundation of China (Project Nos. 20474038 and 50390090) was acknowledged. S.Z. thanks the Shanghai Educational Development Foundation, China, for an award (2004-SG-18) to the "Shuguang Scholar".

References

[1] May CA, Tanaka GY, editors. Epoxy resin chemistry and technology. New York: Marcel Dekker; 1973.
[2] Bauer RS, editor. Advances in chemistry series, vol. 114. Washington, DC: American Chemical Society; 1979.
[3] Manson JA, Hertzberg RW, Connelly GM, Hwang J. In: Paul DR, Sperling LM, editors. Multi-component polymer materials. Advances in chemistry series, vol. 211; 1986. p. 300.
[4] Sultanm JN, McGarry FJ. Polym Eng Sci 1973;13:29.
[5] Riew CK, Rowe EH, Siebert AR. Am Chem Soc Adv Chem Ser 1976;154:326.
[6] Kunz SC, Sayre JA, Assink R. Polymer 1973;23:1897.
[7] Yee AF, Pearson RA. J Mater Sci 1986;21:2462.
[8] Yorkgitis EM, Eiss NS, Tran C, Wilkes GL, McGrath LE. Am Chem Soc Adv Polym Sci 1985;72:70.
[9] Meijerink JI, Eguchi S, Ogata M, Ishii T, Amagi S, Numata S, et al. Polymer 1994;35:179.
[10] Zheng S, Wang H, Dai Q, Luo X, Ma D. Macromol Chem Phys 1995;196:269.
[11] Kemp TJ, Wilford A, Howarth OW, Lee TCP. Polymer 1992;33:1860.
[12] Hisich HSY. Polym Eng Sci 1990;30:493.

[13] Bussi P, Ishida H. J Appl Polym Sci 1994;32:647.
[14] Kumar RS, Alagar M. J Appl Polym Sci 2006;101:668.
[15] Thomas R, Durix S, Sinturel C, Omonov T, Goossens S, Groeninckx G, et al. Polymer 2007;48:1695.
[16] Bucknall CB, Patridge IK. Polymer 1983;24:639.
[17] Bucknall CB, Gilbert AH. Polymer 1989;30:213.
[18] Hourston DJ, Lane JM. Polymer 1992;33:1397.
[19] Hedrick JH, Yilgor I, Jurek M, Hedrick JC, Wilkens GL, McGrath JE. Polymer 1991;13:2020.
[20] Raghava RS. J Polym Sci Part B Polym Phys 1988;26:65.
[21] Gilbert AH, Bucknall CB. Makromol Chem Macromol Symp 1991;45:289.
[22] Cho JB, Hwang JW, Cho K, An JH, Park CE. Polymer 1993;34:4832.
[23] Iijima T, Tochiomoto T, Tomoi M. J Appl Polym Sci 1991;63:311.
[24] Zheng S, Wang J, Guo Q, Wei J, Li J. Polymer 1996;37:4667.
[25] Takahashi T, Nakajima N, Saito N. In: Riew CK, editor. Rubber-toughened plastics. Advances in chemistry series, vol. 222. Washington, DC: Am Chem Soc; 1989.
[26] Pascault JP, Williams RJJ. In: Paul DR, Bucknall CB, editors. Polymer blends, vol. 1. New York: Wiley; 2000. p. 379–415.
[27] Hillmyer MA, Lipic PM, Hajduk DA, Almdal K, Bates FS. J Am Chem Soc 1997;119:2749.
[28] Lipic PM, Bates FS, Hillmyer MA. J Am Chem Soc 1998;120:8963.
[29] Mijovic J, Shen M, Sy JW, Mondragon I. Macromolecules 2000;33:5235.
[30] Francis B, Rao VL, Poel GV, Posada F, Groenincks G, Ramaswamy R, et al. Polymer 2006;47:5411.
[31] Francis B, Thomas S, Jose J, Ramaswamy R, Rao VL. Polymer 2005;46:12372.
[32] Guo Q, Thomann R, Gronski W. Macromolecules 2002;35:3133.
[33] Guo Q, Thomann R, Gronski W. Macromolecules 2003;36:3635.
[34] Fan HB, Yuen MMF. Polymer 2007;48:2174.
[35] Yang G, Fu S-Y, Yang J-P. Polymer 2007;48:302.
[36] Wu C, Xu W. Polymer 2006;47:6004.
[37] Lee J, Yandek GP, Kyu T. Polymer 2005;46:12511.
[38] Ritzenthaler S, Court F, Girard-Reydet E, Leibler L, Pascault JP. Macromolecules 2002;35:6245.
[39] Ritzenthaler S, Court F, Girard-Reydet E, Leibler L, Pascault JP. Macromolecules 2003;36:118.
[40] Kosonen H, Ruokolainen J, Nyholm P, Ikkala O. Macromolecules 2001;34:3046.
[41] Kosonen H, Ruokolainen J, Nyholm P, Ikkala O. Polymer 2001;42:9481.
[42] Grubbs RB, Dean JM, Broz ME, Bates FS. Macromolecules 2000;33:9522.
[43] Rebizant V, Abetz V, Tournihac T, Court F, Leibler L. Macromolecules 2003;36:9889.
[44] Dean JM, Verghese NE, Pham HQ, Bates FS. Macromolecules 2003;36:9267.
[45] Rebizant V, Venet AS, Tournillhac F, Girard-Reydet E, Navarro C, Pascault JP, et al. Macromolecules 2004;37:8017.
[46] Dean JM, Grubbs RB, Saad W, Cook RF, Bates FS. J Polym Sci Part B Polym Phys 2003;41:2444.
[47] Wu J, Thio YS, Bates FS. J Polym Sci Part B Polym Phys 2005;43:1950.
[48] Maiez-Tribut S, Pascault JP, Soule ER, Borrajo J, Williams RJJ. Macromolecules 2007;40:1268.
[49] Sinturel C, Vayer M, Erre R, Amenitsch H. Macromolecules 2007;40:2532.
[50] Larrañaga M, Gabilondo N, Kortaberria G, Serrano E, Remiro P, Riccardi CC, et al. Polymer 2005;46:7082.
[51] Meng F, Zheng S, Zhang W, Li H, Liang Q. Macromolecules 2006;39:711.
[52] Meng F, Zheng S, Li H, Liang Q, Liu T. Macromolecules 2006;39:5072.
[53] Meng F, Zheng S, Liu T. Polymer 2006;47:7590.
[54] Serrano E, Tercjak A, Kortaberria G, Pomposo JA, Mecerreyes D, Zafeiropoulos NE, et al. Macromolecules 2006;39:2254.
[55] Xu Z, Zheng S. Macromolecules 2007;40:2548.
[56] Buchholz U, Mülhaupt R. Polym Prepr 1992;33:205.
[57] Könczöl L, Döll W, Buchholz U, Mülhaupt R. J Appl Polym Sci 1994;54:815.
[58] Guo Q, Chen F, Wang K, Chen L. J Polym Sci Part B Polym Phys 2006;44:3402.
[59] Yin M, Zheng S. Macromol Chem Phys 2005;206:929.
[60] Ni Y, Zheng S. Polymer 2005;46:5828.
[61] Sanja ZN, Kupehela L. Polym Eng Sci 1976;28:1149.
[62] Ochi M, Okasaki M, Shimbo M. J Polym Sci Part B Polym Phys 1982;20:89.
[63] Shibanov YD, Godovsky YK. Prog Colloid Polym Sci 1989;80:110.